



## Research Article

# Localization of $\text{Na}^+ \text{-} \text{K}^+$ -ATPase and $\text{Na}^+ \text{-} \text{K}^+$ - $2\text{Cl}^-$ cotransporter, and $\text{Na}^+ \text{-} \text{H}^+$ exchanger in the renal system of Walton's mudskipper (*Periophthalmus waltoni*) using immunohistochemistry and histology methods

Esfandiyari K.<sup>1</sup>; Babaei M.<sup>2</sup>; Morovvati H.<sup>1</sup>; Tarabi A.M.<sup>3</sup>;  
Kalantari-Hesari A.<sup>4\*</sup>

Received: March 2022

Accepted: July 2022

## Abstract

Kidneys play an important role in regulating the balance of water and ions in freshwater and seawater fish. However, complex kidney structures impair a comprehensive understanding of kidney function. In this study, in addition to the investigation of renal histology,  $\text{Na}^+ \text{-} \text{K}^+$ -ATPase,  $\text{Na}^+ \text{-} \text{K}^+$ - $2\text{Cl}^-$  cotransporter (NKCC), and  $\text{Na}^+ \text{-} \text{H}^+$  exchanger (NHE) were localized in the renal system of Walton's mudskipper (*Periophthalmus waltoni*). The kidney samples were fixed and they passed the preparing section and staining stages. The renal tubules were composed of proximal tubules and distal tubules, followed by collecting tubes and finally collecting ducts. The distribution of the  $\text{Na}^+ \text{-} \text{K}^+$ -ATPase immune response varied in different sections of the nephron. The NKCC positioning was reported only in collecting tubes and collecting ducts, and proximal tubes and distal tubes did not respond to the antibody. Immunohistochemical response for NHE3 localization was detected only at the apex of epithelial cells of proximal tubules and collecting tubes. The distal tubes showed a negative reaction and the collecting ducts showed a weak response to NHE3 immunolocalization. In conclusion,  $\text{Na}^+ \text{-} \text{K}^+$ -ATPase, NKCC, and NHE were differentially located in the renal system, suggesting that various physiological system operates in the renal system for ionic retention. This study provided valuable information to understand the ion regulation abilities of epithelial cells in various parts of *P. waltoni* nephrons.

**Keywords:** *Periophthalmus*, Nephrons tubules, Ionic retention, Antibody, Kidney

1-Department of Basic Science, Faculty of Veterinary Medicine, University of Tehran, Tehran, Iran.

2-Department of Clinical Sciences, Faculty of Veterinary Science, Bu-Ali Sina University, Hamedan, Iran.

3-Food industry science and engineering, Islamic azad university- Tehran north branch, Tehran, Iran.

4-Department of Pathobiology, Faculty of Veterinary Science, Bu-Ali Sina University, Hamedan, Iran.

\*Corresponding author's Email: a.kalantarihesari@basu.ac.ir

## Introduction

Several teleost fish species have developed strategies for maintaining fluid and electrolyte homeostasis across a wide range of salinities, involving integrated ion and kidney water transport activities. About 3 to 5% of teleosts are euryhaline and have ability to acclimate to strongly hypotonic and hypertonic salinities. The anatomic and physiological knowledge of the cooperative osmoregulatory functions of the gills, kidneys and intestine are numerous. Hence, major reviews have focused on renal physiology in FW and SW acclimated fishes (Takvam *et al.*, 2021).

The urinary system in fish consists of renal-corpuscles, proximal tubules, distal tubules, collecting tubules, and collecting ducts. While the mechanism of ion retention restricts the leakage of ions across the epithelium, ion acquisition compensates for ions lost by the epithelium. Studies examining the ion regulation role of the epithelium in maintaining hydromineral homeostasis in fish have generally focused on intracellular mechanisms including ion pathways through which active ion transport occurs (Gonçalves *et al.*, 2016; Shaughnessy and Breves, 2021). In contrast, less emphasis has been placed on ion retention mechanisms that limit ion loss by cells. When identifying intercellular pathways, multifaceted assemblies of ion pumps, transducers, and channels linked with the apical or basolateral membrane of the cell have been identified (Marshall, 2002; Evans *et al.*, 2005; Alves *et al.*, 2019).

Intercellular pathways controlled by tight junctions between two cells have not been well understood in aquatic vertebrates. Proteins involved in the tight junctions of adjacent epithelial cells communicate with each other and restrict the movement of solutes between cells (Anderson and Van Itallie, 2009).

Sodium transmission through renal and intestine epithelium as well as body surface is a major system by which  $\text{Na}^+$  homeostasis is regulated in fish. There is scarce information about the  $\text{Na}^+$  carriers responsible for  $\text{Na}^+$  homeostasis in bony fish.

NHE3 is located in the brush border (apical) of the intestinal epithelial membrane (jejunum, ileum, and colon) and in the renal tubules (proximal tubule and distal straight *tubule of Henle's loop*). NHE3 is found in the apical membrane of ionocytes in the gills of both freshwater and seawater fish. Since the gills are the major site of ion regulation in fish (Choe *et al.*, 2005), NHE3 may facilitate  $\text{Na}^+$  uptake and  $\text{H}^+$  secretion in fish gills. However, NHE3 is known as a  $\text{Na}^+ \text{-} \text{H}^+$  exchanger that can leak intracellular  $\text{Na}^+$  intermediates into fresh ambient water (Esaki *et al.*, 2007; Lin *et al.*, 2008).

NHEs catalyze the electrical and neutral exchange of  $\text{Na}^+$  and  $\text{H}^+$  (1:1 ratio) in the corresponding concentration gradient (Hayashi *et al.*, 2002). NHE2 and NHE3 are expressed in the apical membrane of gastrointestinal and kidney cells of rat model, where they can participate in the systematic uptake of  $\text{Na}^+$  and  $\text{H}^+$  secretion. In the kidney, NHE2 is found in the thick ascending

limb of the loop of Henle, macula densa, distal convoluted tubules, and the collecting tubules (Chambrey *et al.*, 1998). NHE3 is found mainly in the proximal convoluted tubule and to a lesser extent in the thick ascending limb of shark kidney (Biemesderfer *et al.*, 1996). In mammalian proximal renal tubules, apical NHE3 interacts with  $\text{Na}^+ \text{-K}^+$ -ATPase and  $\text{Na}^+ \text{-HCO}_3$  cotransporter channels in a mechanism responsible for the reabsorption of sodium and  $\text{HCO}_3$  in the rat kidney (Vallon *et al.*, 2000).

Walton's mudskipper genus from the Gobiidae family is the largest family of fish after the carp. The Walton's mudskipper often inhabits saltwater and are highly morphologically, behaviorally, and ecologically diverse. Most species are predators and have adapted to living in the shallow waters of the oceans, seas, and lakes. Among the three species of mudskippers, Walton's mudskipper is native to the Persian Gulf and the Oman Sea. Walton's mudskipper is of little economic value, but is a popular food for people in China, Korea, Japan, and Taiwan, and is prey for terrestrial and aquatic animals, including birds and fish in its habitat (Maghsodian *et al.*, 2021; Kerdgari *et al.*, 2022).

In this study, in addition to the investigation of renal histology,  $\text{Na}^+ \text{-K}^+$ -ATPase, NKCC, and NHE were localized in the renal system of Walton's mudskipper.

### Material and methods

Fifteen adult Walton's mudskippers with an average weight of  $16.76 \pm 0.42$  g and a

length of  $16.62 \pm 1.10$  cm were used in this study. Live samples were purchased from local fishermen of Mahshahr city located in the Persian Gulf. This research performed in accordance with the ethical standards and considerations of the veterinary faculty of Tehran university, Iran, at which the study was conducted. The samples were collected from different parts of the kidney and fixed in 4% paraformaldehyde for 24 h. After tissue processing, the tissue blocks were sectioned at 5–6  $\mu\text{m}$  for immunohistochemical investigations. For this study, the slides were first washed using an Ultrasonic Cleaner machine (Model: JP-030S, Shenzhen company, China) in acid and alcohol solutions with a concentration of 70% HCl and 1% EtOH at 60°C for 15 min. They were then washed in tab water for 15 min and soaked in distilled water for another 15 min. The samples were then left to dry gradually at a temperature of 37°C for 24 h. The slides were then immersed in a solution composed of 245 mL acetone and 5 mL 3-aminoisoquinoline triethoxysilane. After placing tissue incisions on the coated slides, they were immersed in xylene and then in decreasing concentrations of alcohol ending up at 0% alcohol (distilled water). The samples were then boiled in 0.05% citraconic anhydride solution for 30 min before cooling in distilled water for 10 min and drying in an incubator at 37°C for an h. The slides were then immersed in SDS (Sodium dodecyl sulfate) solution for five min and then in TPBS (Tween phosphate buffered saline) solution for 5 to 10 min,

after which 75  $\mu\text{L}$  of blocking buffer was added to each section. The slides were then placed in a damp room. Rabbit  $\alpha\text{R1}$  antibody and rat T4 antibody were used simultaneously on one section as the primary antibodies (anti-rabbit and anti-mouse secondary antibody). After adding

secondary antibodies to each section, the slides were kept at 4°C in a humidified chamber overnight. The slides were rehydrated in TPBS (Gonçalves *et al.*, 2016). Antibodies used in the current research are as Table 1.

**Table 1: Antibodies used in the current research.**

Primary Antibody	Target Enzyme	Animal Type	Dilution	Diluent	Secondary Antibody
$\alpha\text{R1}$	$\text{Na}^+ \text{-} \text{K}^+$ -ATPase	Rabbit	1:500	Blocking buffer	Anti-Rabbit Secondary Antibody
$\alpha\text{5}$	$\text{Na}^+ \text{-} \text{K}^+$ -ATPase	Mouse	1:100	" "	" "
T4	$\text{Na}^+ \text{-} \text{K}^+$ - $2\text{Cl}^-$	Mouse	1:100	" "	" "
NHE3B	$\text{Na}^+ \text{-H}^+$ Exchanger	Rabbit	1:200	" "	" "
Control Group					" "

A secondary antibody (50  $\mu\text{L}$ ) was added to all sections including the control group. A blocking buffer was used to dilute the secondary antibody. For each 500  $\mu\text{L}$  of the solution containing the secondary antibody, 1  $\mu\text{L}$  of the anti-rabbit secondary antibody and 1  $\mu\text{L}$  of anti-mouse secondary antibody were used. After adding 50  $\mu\text{L}$  of secondary antibody to all sections, they were incubated at 37°C (humidified chamber) for an h. The samples were placed in TPBS for 5 min and then mixed with DAPI (60 mL TPBS with 5  $\mu\text{L}$  DAPI). DAPI (4',6-diamidino-2-phenylindole), was used for molecular staining of the nucleus (Gonçalves *et al.*, 2016).

## Results

Macroscopic studies showed that the kidney structures as two reddish-purple extraperitoneal tissues stretched below the spine and covered the roof of the

internal cavity. The encapsulated kidney consisted of loose connective tissue which was covered by a layer of mesothelial cells. As we progress along the kidney from the head to the tail of fish, malpighian bodies were replaced with tubules. Each nephron was made up of the renal tubules and a malpighian body. The malpighian body and the Bowman's capsule were clearly visible (Fig. 1).

Bowman's capsule consisted of a parietal layer which was a simple layer of simple squamous epithelium and a visceral layer of podocytes. Nucleated red blood cells could be identified in the renal sinusoids and hematopoietic parenchyma of the kidney. Proximal convoluted tubules, distal convoluted tubules, collecting tubules, and collecting ducts could be respectively observed in nephron structure. Further observations using immunohistochemical tools showed

physiological properties regarding the uptake and excretion of ions for each section (see below).

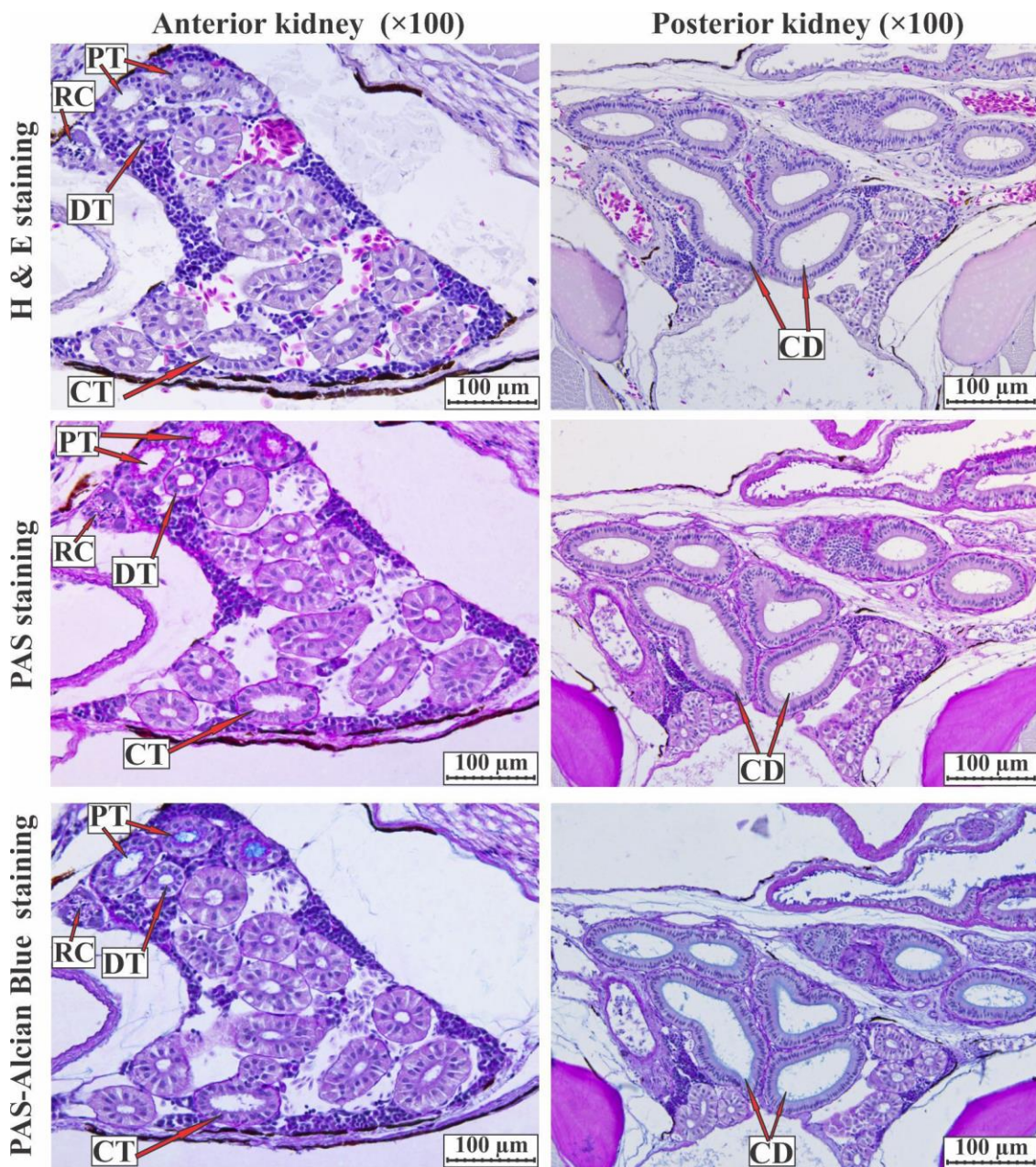


**Figure 1:** Histological section of the anterior and posterior kidney in Walton's mudskipper. Stained with H & E, PAS and PAS-Alcian blue staining. H & E section staining shown that the urinary system was consisted of renal corpuscles (RC), proximal tubules (PT), distal tubules (DT), collecting tubules (CT) and collecting ducts (CD). Positive reaction to PAS staining (in red) was observed in the basement membrane of all tubules and ducts and the apical part of the PTs and relatively less in the DTs. Positive reaction to PAS-Alcian blue staining (light blue) was observed in the apical part of the PTs and CDs.

Light microscope immunohistochemistry was utilized to

localize the  $\text{Na}^+ \text{-K}^+$ -ATPase along renal tubules and collecting tubules. The

distribution of the  $\text{Na}^+/\text{K}^+$ -ATPase immune response was varied in different sections. Basal sections of proximal and distal convoluted tubules showed a positive response to immunolocalization of  $\text{Na}^+/\text{K}^+$ -ATPase, while a negative response in their apical sections was observed. The  $\text{Na}^+/\text{K}^+$ -ATPase existed in all basolateral parts of collecting tubes and collecting ducts and reacted

positively to  $\text{Na}^+/\text{K}^+$ -ATPase immunolocalization.  $\text{Na}^+/\text{K}^+$ -ATPase, which was located in the basal and basolateral portions of the renal tubule's epithelial cells, exchanges three  $\text{Na}^+$  ions with two  $\text{K}^+$  ions to the basal and interstitial tissue of the kidney and into the cell, respectively (Fig. 2).

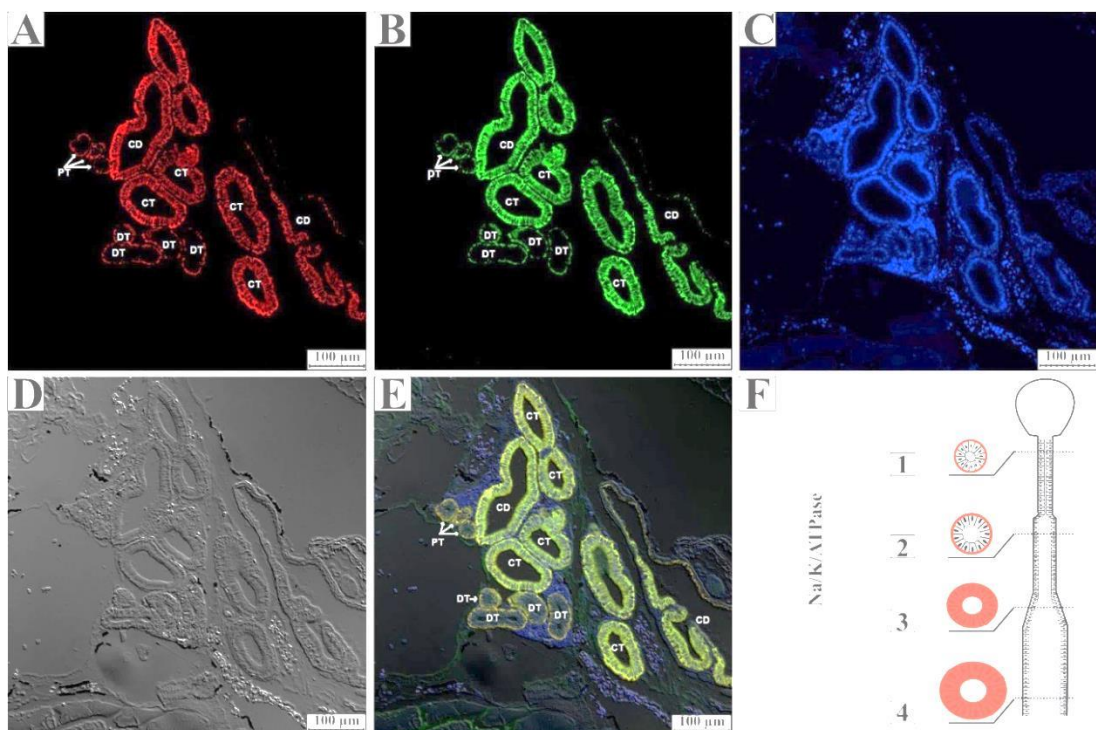


**Figure 2: Double labeling of  $\text{Na}^+/\text{K}^+$ -ATPase enzyme in the renal system of Walton's mudskipper.** (A) immunolocalization of  $\text{Na}^+/\text{K}^+$ -ATPase using  $5\alpha$  antibody (red). (B) immunolocalization of  $\text{Na}^+/\text{K}^+$ -ATPase using  $R1\alpha$  antibody (green). (C) Nuclear staining of kidney tissue using DAPI (blue). (D) The background of entire kidney tissue. (E) Merged images of A-D: In Figures A and B, proximal and distal convoluted tubules reacted positively to  $\text{Na}^+/\text{K}^+$ -ATPase antibodies showed their localizations in basolateral portions and negatively in apical portions.  $\text{Na}^+/\text{K}^+$ -ATPase was existed in all the basal and lateral portions of the collecting tubules and collecting ducts. (F) A schematic view of localization of  $\text{Na}^+/\text{K}^+$ -ATPase in different parts of tubules and ducts (No. 1: proximal tubule; No. 2: distal tubule; No. 3: collecting tubules; No. 4: collecting ducts).

The location of NKCC was recorded only in the basolateral part of epithelial cells with higher intensity in collecting

tubules and lower intensity in collecting ducts (Fig. 3).

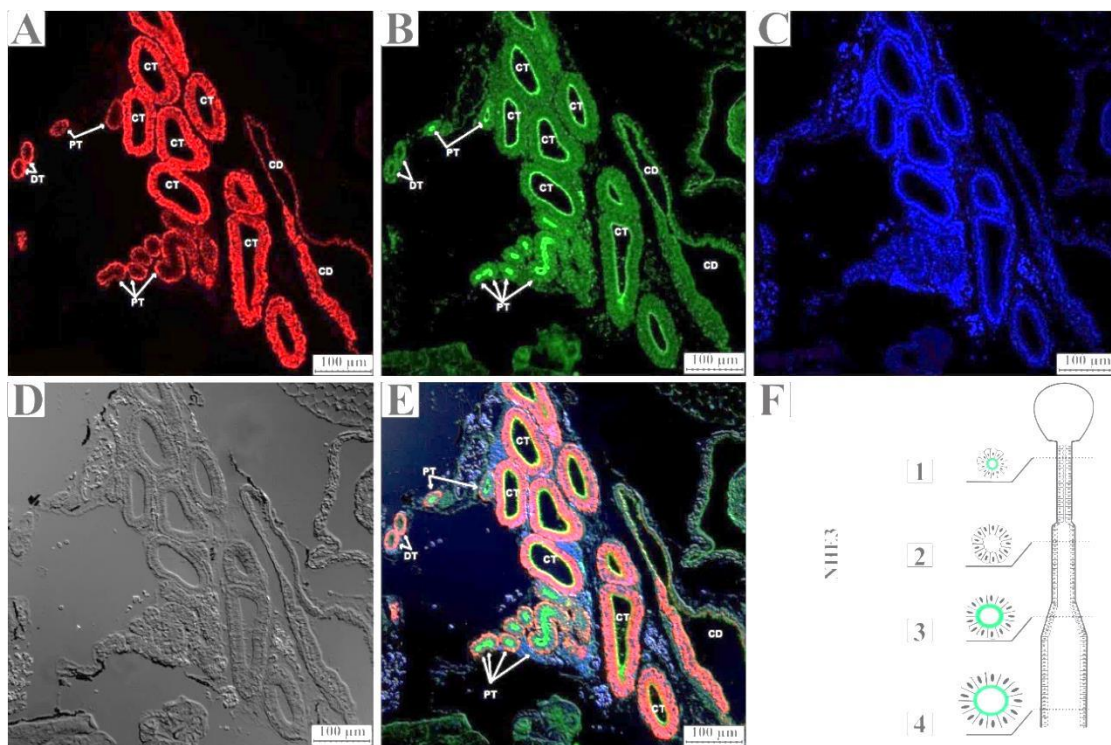


**Figure 3: Double labeling of  $\text{Na}^+-\text{K}^+$ -ATPase and  $\text{Na}^+/\text{K}^+/2\text{Cl}^-$  in the renal system of Walton's mudskipper.** (A) Immunolocalization of  $\text{Na}^+-\text{K}^+-2\text{Cl}^-$  using T4 antibody (red). (B) Immunolocalization of  $\text{Na}^+-\text{K}^+$ -ATPase using R1 $\alpha$  antibody (green). (C) Nuclear staining of kidney tissue using DAPI (blue). (D) The background of entire kidney tissue. (E) Merged images of A-D. In panel A, the  $\text{Na}^+-\text{K}^+-2\text{Cl}^-$  cotransporter was located only at the apex of the epithelial cells in the collecting tubules and to a lesser extent in the collecting ducts. However, the epithelial cells located in the proximal and distal tubules did not respond to the  $\text{Na}^+-\text{K}^+-2\text{Cl}^-$  cotransporter immunolocalization. (F) A schematic view of the stained of different parts of tubule and ducts (No. 1: proximal tubule; No. 2: distal tubule; No. 3: collecting tubules; No. 4: collecting ducts).

This is while epithelial cells located in the proximal and distal tubules did not respond to the NKCC immunolocalization. This protein pumps  $\text{Na}^+$ ,  $\text{K}^+$ , and  $\text{Cl}^-$  ions from the lumen into the epithelial cells. Immunohistochemical reaction for localization of NHE was detected at the apex of the epithelial cells at the proximal tubules, collecting tubes, and

collecting ducts with very high, moderate and low intensities, respectively. Distal tubules did not respond to NHE immunolocalization (Fig. 4). NHE was located at the apex of the cells to mediate  $\text{H}^+$  export from cell to lumen in exchange for the import of one  $\text{Na}^+$  ion into the epithelial cell.

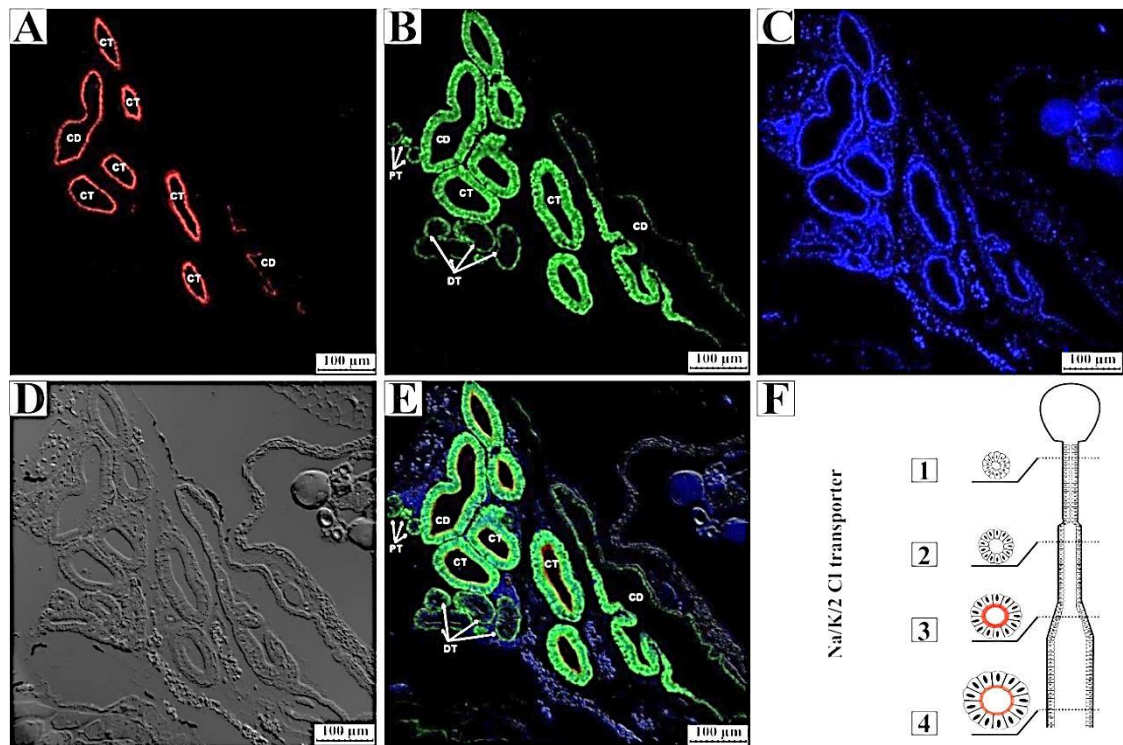


**Figure 4: Double labeling of  $\text{Na}^+ \text{-H}$  Exchanger (NHE) and  $\text{Na}^+ \text{-K}^+$ -ATPase in the renal system of Walton's mudskipper.** (A) Immunolocalization of  $\text{Na}^+ \text{-K}^+$ -ATPase using  $\alpha 5$  antibody (red). (B) Immunolocalization of NHE using NHE3b antibody (green). (C) Nuclear staining of kidney tissue using DAPI (blue). (D) The background the entire of kidney tissue. (E) Merged images of A-D. Immunohistochemical activity for NHE localization was detected only at the apex of epithelial cells of proximal tubules, collecting tubules and collecting ducts with high, moderate and low intensities, respectively. The distal tubules did not respond to NHE immunolocalization. (F) A schematic view of the stained of different parts of tubule and ducts (No. 1: proximal tubule; No. 2: distal tubule; No. 3: collecting tubules; No. 4: collecting ducts).

## Discussion

Differential immunohistochemical staining of  $\text{Na}^+ \text{-K}^+$ -ATPase has been carried out in different sections of goldfish (*Carassius auratus auratus*) nephrons and other fish species (Chasiotis *et al.*, 2012). The basolateral localization of  $\text{Na}^+ \text{-K}^+$ -ATPase has been reported for ion transports (Piepenhagen *et al.*, 1995; Kwon *et al.*, 1998; Sturla *et al.*, 2003). In goldfish kidney, immunostaining response for  $\text{Na}^+ \text{-K}^+$ -ATPase is primarily restricted to the basement membrane of renal epithelial cells in the proximal region of the nephron as well as the basolateral

membrane of renal epithelial cells in the distal and collecting tubules (Chasiotis *et al.*, 2012). In the current study, the expression of  $\text{Na}^+ \text{-K}^+$ -ATPase was verified in all sections of nephron tubules. Therefore, the localization of  $\text{Na}^+ \text{-K}^+$ -ATPase is different in the nephron structure of various species.

Interestingly, in both killifish (*Fundulus heteroclitus*) and rainbow trout (*Oncorhynchus mykiss*), compatibility with freshwater or seawater environments does not cause immunohistochemical changes in the kidney at the microscopic level either for light or electron microscopy (Katoh *et*

al., 2008). Two important NKCC isoforms, including the NKCC1 secretory form and the NKCC2 absorption form, can be found in vertebrates. In dogfish kidneys, however, the basolateral isoform (NKCC1) has been observed which is distributed in the proximal tubules while the NKCC2 isoform is observed apically from the proximal tubules to the collecting tubules (Biemesderfer *et al.*, 1996). Secretory isoform (NKCC1) has also been found basolaterally in the large rectum of fish (Lytle *et al.*, 1992). The anti-NKCC antibody used in the present study (T4) detects both secretory and absorption isoforms in a variety of animal tissues (Lytle *et al.*, 1992). Therefore, in the present study, we cannot distinguish between these isoforms in different regions of the nephron. Katoh *et al.* (2008) Suggested that in the rainbow trout kidney only NKCC2 is present and located apically, while in the killifish kidney NKCC2 isoform is present apically and the NKCC1 isoform is present basolaterally. NKCC is present basally in the first and second parts of the proximal tubule where they pump ions from interstitial tissue into epithelial cells, while in the distal and collecting tubules NKCC is present in the apical part of the cells and pumps ions from the lumen into the epithelial cells.  $\text{Na}^+ \text{-K}^+$ -ATPase is also present basolaterally in the second part of the proximal tubule as well as distal tubules and collecting tubules. NKCC was only reported apically in the distal and collecting tubules (Katoh *et al.*, 2008). In the present study, detection of

$\text{Na}^+ \text{-K}^+$ -2Cl<sup>-</sup> expression was limited to collecting tubules and collecting ducts with higher intensities in the latter.

The NHE3 is located in the apical membrane ionocytes in the gills of freshwater fish and seawater fish (Choe *et al.*, 2005). Immunohistochemically localization of NHE3 responded positively in the brush border of intestinal epithelium (jejunum, ileum, and colon) and in the renal tubules (proximal tubule and thick ascending limb) (Mahnensmith and Aronson, 1985).

In a study carried out by Katoh *et al.* (2008). on the expression of the third isoform of NHE in *Triakis scyllium*, the kidneys were divided into bundle and sinus regions from an immunohistochemical viewpoint.

In fixed sections of the *Triakis* kidney, NHE3-specific signals were detected in the apical membrane of the renal tubules in both the bundle and sinus regions. In the sinus region of the *Triakis* kidney, specific signals for NHE3 were detected in part of the proximal as well as the end of distal tubules. In other words, the NHE3 was both positive and observed in both tubules. NHE3-negative proximal tubes were often observed in the sinusoidal region near the bundle region. In the bundle region, the five tubular sections are placed side by side to conduct the flow and are separated by a sheath from the adjacent bundle region. NHE3-specific signals were found in the apical membrane of one of the five tubes. The NHE3 in Japanese banded houndshark (*Triakis scyllium*) is most highly

expressed in the gill, kidney, spiral intestine, and rectum. The NHE3-positive tubes were detected in the bundle area with relatively large diameters consisting of long epithelial cells with no brush border and reacted strongly to  $\text{Na}^+ \text{-} \text{K}^+$ -ATPase localization. These results clearly indicate that NHE3 is expressed in the first part of the distal tubule (Li *et al.*, 2013).

In conclusion, it can be said that NHE expression became detected best on the apex of epithelial cells of the proximal tubules, collecting tubes and collecting ducts with high, moderate, and low intensities, respectively, whilst distal tubules did not react to NHE immunolocalization.

## Abbreviations

SDS: Sodium dodecyl sulfate; TPBS: Tween phosphate buffered saline; DAPI: 4',6-diamidino-2-phenylindole; NHE:  $\text{Na}^+ \text{-} \text{H}^+$  Exchanger; NKCC:  $\text{Na}^+ \text{-} \text{K}^+$ - $2\text{Cl}^-$  cotransporter.

## Acknowledgements

Authors gratefully acknowledge the help of Tehran University in this study.

## References

**Alves, A., Gregório, S.F., Egger, R.C. and Fuentes, J., 2019.** Molecular and functional regionalization of bicarbonate secretion cascade in the intestine of the European sea bass (*Dicentrarchus labrax*). *Comparative Biochemistry and Physiology Part A: Molecular & Integrative Physiology*, 233, 53-64. DOI: 10.1016/j.cbpa.2019.03.017.

**Anderson, J.M. and Van Itallie, C.M., 2009.** Physiology and function of the tight junction. *Cold Spring Harbor perspectives in biology*, 1(2), a002584. DOI: 10.1101/cshtperspect.a002584.

**Biemesderfer, D., Payne, J.A., Lytle, C.Y. and Forbush, B., 1996.** Immunocytochemical studies of the  $\text{Na} \text{-} \text{K} \text{-} \text{Cl}$  cotransporter of shark kidney. *American Journal of Physiology*, 270(6), 927-936. DOI: 10.1152/ajprenal.1996.270.6.F927.

**Chambrey, R., Warnock, D.G., Podevin, R.A., Bruneval, P., Mandet, C., Bélair, M.F., Bariéty, J. and Paillard, M., 1998.** Immunolocalization of the  $\text{Na}^+ \text{-} \text{H}^+$  exchanger isoform NHE2 in rat kidney. *American Journal of Physiology*, 275(3), 379-386. DOI: 10.1152/ajprenal.1998.275.3.F379.

**Chasiotis, H., Kolosov, D. and Kelly, S.P., 2012.** Permeability properties of the teleost gill epithelium under ion-poor conditions. *American Journal of Physiology-Regulatory, Integrative and Comparative Physiology*, 302(6), 727-739. DOI: 10.1152/ajpregu.00577.2011.

**Choe, K.P., Kato, A., Hirose, S., Plata, C., Sindic, A., Romero, M.F., Claiborne, J.B. and Evans, D.H., 2005.** NHE3 in an ancestral vertebrate: primary sequence, distribution, localization, and function in gills. *American Journal of Physiology-Regulatory, Integrative and Comparative Physiology*, 289(5), 1520-1534. DOI: 10.1152/ajpregu.00048.2005.

**Esaki, M., Hoshijima, K., Kobayashi, S., Fukuda, H., Kawakami, K. and Hirose, S., 2007.** Visualization in zebrafish larvae of Na (+) uptake in mitochondria-rich cells whose differentiation is dependent on foxi3a. *American Journal of Physiology-Regulatory, Integrative and Comparative Physiology*, 292(1), 470-480. DOI: 10.1152/ajpregu.00200.2006.

**Evans, D.H., Piermarini, P.M. and Choe, K.P., 2005.** The multifunctional fish gill: dominant site of gas exchange, osmoregulation, acid-base regulation, and excretion of nitrogenous waste. *Physiological Reviews*, 85(1), 97-177. DOI: 10.1152/physrev.00050.2003.

**Gonçalves, O., Castro, L.F., Smolka, A.J., Fontainhas, A. and Wilson, J.M., 2016.** The gastric phenotype in the cypriniform loaches: a case of reinvention? *PLoS One*, 11(10), e0163696. DOI: 10.1371/journal.pone.0163696.

**Hayashi, H., Szászi, K. and Grinstein, S., 2002.** Multiple modes of regulation of  $\text{Na}^+/\text{H}^+$  exchangers. *Annals of the New York Academy of Sciences*, 976(1), 248-258. DOI: 10.1111/j.1749-6632.2002.tb04747.x.

**Katoh, F., Cozzi, R.R., Marshall, W.S. and Goss, G.G., 2008.** Distinct  $\text{Na}^+/\text{K}^+/2\text{Cl}^-$  cotransporter localization in kidneys and gills of two euryhaline species, rainbow trout and killifish. *Cell and Tissue Research*, 334(2), 265-281. DOI: 10.1007/s00441-008-0679-4.

**Kerdgari, M., Afkhami, M., Ehsanpour, M. and Ghanbarzadeh, M., 2022.** Monitoring anthropogenic pollutants in northern coasts of Hormuz Strait using blood indices and thyroid hormone levels in *Periophthalmus argenteolineatus* (Pisces: Gobiidae). *Iranian Journal of Fisheries Sciences*, 21(2), 431-444. DOI: 10.22092/ijfs.2022.350699.0.

**Kwon, O., Myers, B.D., Sibley, R., Dafoe, D., Alfrey, E. and Nelson, W.J., 1998.** Distribution of cell membrane-associated proteins along the human nephron. *Journal of Histochemistry and Cytochemistry*, 46(12), 1423-1434. DOI: 10.1177/002215549804601211.

**Li, S., Kato, A., Takabe, S., Chen, AP., Romero, MF., Umezawa, T., Nakada, T., Hyodo, S. and Hirose, S., 2013.** Expression of a novel isoform of  $\text{Na}^+/\text{H}^+$  exchanger 3 in the kidney and intestine of banded houndshark, *Triakis scyllium*. *American Journal of Physiology-Regulatory, Integrative and Comparative Physiology*, 304(10), 865-876. DOI: 10.1152/ajpregu.00417.2012.

**Lin, TY., Liao, BK., Horng, J.L., Yan, J.J., Hsiao, C.D. and Hwang, P.P., 2008.** Carbonic anhydrase 2-like a and 15a are involved in acid-base regulation and  $\text{Na}^+$  uptake in zebrafish  $\text{H}^+$ -ATPase-rich cells. *American Journal of Physiology-Cell Physiology*, 294(5), 1250-1260. DOI: 10.1152/ajpcell.00021.2008.

**Lytle, C., Xu, J.C., Biemesderfer, D., Haas, M. and Forbush, B., 1992.** The  $\text{Na} \text{-} \text{K} \text{-} \text{Cl}$  cotransport protein of shark rectal gland. I. Development of monoclonal antibodies, immunoaffinity purification, and partial biochemical characterization. *Journal of Biological Chemistry*, 267(35), 25428-25437. DOI: 10.1016/S0021-9258(19)74059-9.

**Maghsodian, Z., Sanati, A.M., Ramavandi, B., Ghasemi, A. and Sorial, G.A., 2021.** Microplastics accumulation in sediments and *Periophthalmus waltoni* fish, mangrove forests in southern Iran. *Chemosphere*, 264, 128543. DOI: 10.1016/j.chemosphere.2020.128543

**Mahnensmith, R.L. and Aronson, P.S., 1985.** The plasma membrane sodium-hydrogen exchanger and its role in physiological and pathophysiological processes. *Circulation Research*, 56(6), 773-788. DOI: 10.1161/01.res.56.6.773.

**Marshall, W.S., 2002.**  $\text{Na}^+$ ,  $\text{Cl}^-$ ,  $\text{Ca}^{2+}$  and  $\text{Zn}^{2+}$  transport by fish gills: retrospective review and prospective synthesis. *Journal of Experimental Zoology*, 293(3), 264-283. DOI: 10.1002/jez.10127.

**Piepenhagen, P.A., Peters, L.L., Lux, S.E. and Nelson, W.J., 1995.** Differential expression of  $\text{Na}^+ \text{-} \text{K}^+$ -ATPase, ankyrin, fodrin, and E-cadherin along the kidney nephron. *American Journal of Physiology*, 269(6), 1417-1432. DOI: 10.1152/ajpcell.1995.269.6.C1417.

**Shaughnessy, C.A. and Breves, J.P., 2021.** Molecular mechanisms of  $\text{Cl}^-$  transport in fishes: New insights and their evolutionary context. *Journal of Experimental Zoology Part A: Ecological and Integrative Physiology*, 335(2), 207-216. DOI: 10.1002/jez.2428.

**Sturla, M., Prato, P., Masini, M.A. and Uva, B.M., 2003.** Ion transport proteins and aquaporin water channels in the kidney of amphibians from different habitats. *Comparative Biochemistry and Physiology*, 136(1), 1-7. DOI: 10.1016/s1532-0456(03)00141-8.

**Takvam, M., Wood, C.M., Kryvi, H. and Nilsen, T.O., 2021.** Ion transporters and osmoregulation in the kidney of teleost fishes as a function of salinity. *Frontiers in Physiology*, 12, 664588. DOI: 10.3389/fphys.2021.664588

**Vallon, V., Schwark, J.R., Richter, K. and Hropot, M., 2000.** Role of  $\text{Na}^+ \text{/} \text{H}^+$  exchanger NHE3 in nephron function: micropuncture studies with S3226, an inhibitor of NHE3. *American Journal of Physiology-Renal Physiology*, 278(3), 375-379. DOI: 10.1152/ajprenal.2000.278.3.F375.